

Fast Wavelength-Tunable Lasers on Silicon

Sören Dhoore, *Member, IEEE*, Gunther Roelkens, *Member, IEEE*, and Geert Morthier, *Senior Member, IEEE*

(Invited Paper)

Abstract—We present our recent progress in the realization of heterogeneously integrated InP-on-silicon wavelength-tunable lasers that allow for fast, electronic wavelength tuning. Experimental demonstrations of discretely tunable arrayed waveguide grating (AWG) lasers with filtered feedback and continuously tunable twin-guide (TTG) distributed feedback (DFB) lasers are discussed. Excellent static and dynamic laser characteristics are achieved, with mW-level waveguide-coupled output powers, single-mode operation across the tuning range and direct modulation above 10 Gbit/s. Measured wavelength switching times are less than a few nanoseconds, providing interesting prospects for optical packet switching applications. It is furthermore shown that a novel TTG distributed Bragg reflector (DBR) laser design could further improve the wavelength tuning ranges and efficiencies obtained so far.

Index Terms—Silicon photonics, heterogeneous integration, tunable lasers, AWG laser, filtered feedback, DFB laser, DBR laser, fast wavelength tuning, optical packet switching, wavelength routing.

I. INTRODUCTION

WAVELENGTH-tunable laser diodes are essential components for a wide range of applications and systems in optical communication. Optical packet switching (OPS) is believed to offer a viable solution to sustain the ever-increasing demand for bandwidth in communication networks that are dominated by packet-based internet protocol (IP) traffic. Data center networks are the most notable examples, where the annual global IP traffic is expected to reach more than 20 ZB by 2021, up from less than 7 ZB in 2016 [1]. Common routing implementations are based on electronic packet switching (EPS), which not only cause severe power consumption issues but also increase cabling complexity and operational costs in modern data centers [2]–[4]. In OPS, user data is transmitted in optical packets that are switched entirely in the optical domain, without power-hungry optical-to-electrical conversions and where each optical packet carries its own routing information with it. At the core of an optical packet switch lies the switch technology that is capable of fast data reconfiguration to support a continuous stream of packets with small inter-packet gaps. Packet durations have lengths of 10 to 100 ns. Depending on the bitrate, wavelength switching times of a few nanoseconds to less than 1 ns are hence required. The feasibility of OPS as networking technique thus greatly depends on the availability of high-speed and fast tunable optical transmitters with (sub-) nanosecond switching times and good power efficiency [5].

S. Dhoore, G. Roelkens and G. Morthier are with the Photonics Research Group, Department of Information Technology (INTEC), Ghent University, Gent, B-9052, Belgium. e-mail: Soren.Dhoore@UGent.be.

Manuscript received April 19, 2005; revised August 26, 2015.

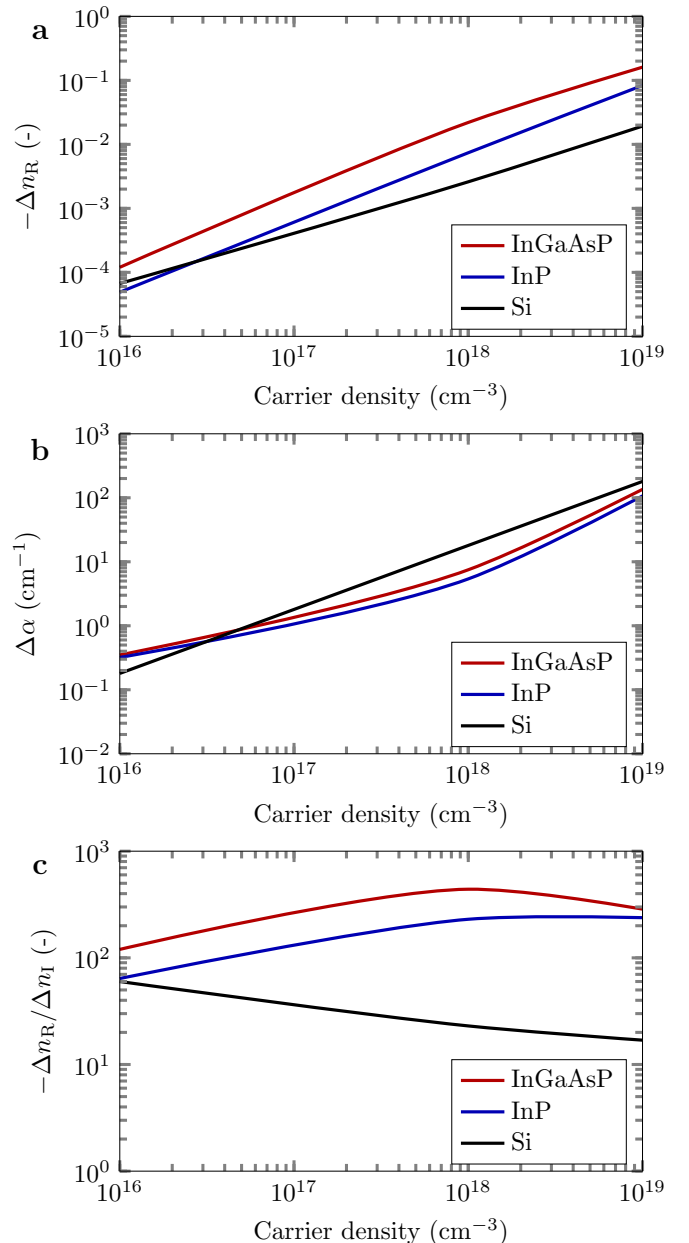


Fig. 1. Free-carrier plasma dispersion effect for InGaAsP, InP and Si. (a) Carrier-induced refractive index change ($-\Delta n_R$); (b) Carrier-induced absorption change ($\Delta\alpha$); (c) $-\Delta n_R/\Delta n_I$ as a function of carrier density.

The silicon (Si) photonics or silicon-on-insulator (SOI) platform has become one of the most promising platforms for photonic integrated circuits (PICs) because of its high index contrast, which results in highly confined waveguide modes and which allows for tight integration with waveguide radii

of only a few μm . Excellent passive functionality and small footprint are therefore the key assets of the SOI platform. Performant fiber-to-chip grating couplers [6], Bragg gratings [7], high-Q ring resonators [8] and arrayed waveguide gratings (AWGs) [9] have already been demonstrated on SOI several years ago. In the meanwhile, silicon photonics has reached a level of maturity that is required for high-volume commercial applications [10].

An important problem of the silicon photonics platform remains the lack of an on-chip light source [11]. Silicon has an indirect bandgap and therefore does not allow efficient light generation, let alone laser operation. In the past decade there has therefore been considerable research in the area of heterogeneous (or hybrid) III-V-on-silicon integration, where III-V lasers are integrated on passive SOI PICs, with light outcoupling to a silicon waveguide [12]–[14]. So far, a wide range of tunable III-V-on-silicon lasers have been demonstrated already. The research has mainly been directed towards thermally tunable lasers since these types typically yield a narrow emission linewidth, a feature that is essential for coherent optical communication [15]. State-of-the-art thermally tunable lasers are based on double-ring configurations in combination with heaters and Sagnac loop mirrors [16] or based on thermally tunable Bragg gratings [17]–[19]. Although useful for an abundance of applications, even beyond optical communication, their tuning speed is too low (with wavelength switching times around $10\ \mu\text{s}$) to find application in OPS systems.

Electronically tunable lasers make use of an extra control current and in principle allow for fast wavelength tuning. However, they are not straightforward to implement on SOI. One of the reasons is that the free-carrier plasma dispersion (FCD) effect used to realize electronic wavelength tuning is about a factor 10 weaker for Si than for typical InP/InGaAsP compounds [20]. The first electronically tunable laser on silicon was presented shortly after the first III-V-on-silicon DFB laser. With a sampled grating (SG-) DBR laser, discrete wavelength tuning was realized. Through quantum well intermixing, passive longitudinal InP-grating sections with different bandgaps were created, allowing current injection to tune the laser wavelength [21]. Tuning was, however, discrete and only two supermodes were addressed because of the limited electronic effect. More recently, a III-V-on-silicon laser with integrated intracavity metal-oxide-semiconductor (MOS) capacitor formed between a heavily doped InGaAsP and doped silicon waveguide layer allowed for electronic wavelength control [22]. Such an approach has the advantage of low thermal chirp and power consumption. The demonstrated tuning range was limited to 0.4 nm, however, and the side-mode suppression ratio (SMSR) was lower than 18 dB across the tuning range. In other work [23], a fast tunable laser was demonstrated based on double-ring silicon resonators with lateral *p-i-n* junctions. However, fast wavelength switching was limited to neighboring channels, owing to silicon's weak FCD effect.

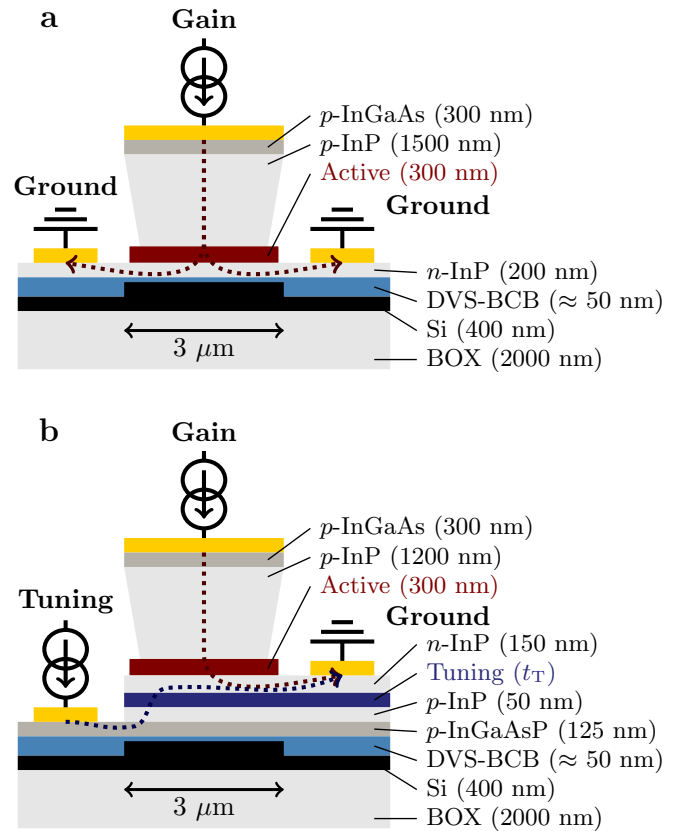


Fig. 2. Waveguide cross-sections of the considered heterogeneously integrated laser structures. (a) Standard InP stack; (b) TTG InP stack.

II. FAST WAVELENGTH TUNING ON SILICON

The FCD effect essentially involves the refractive index change $\Delta n = \Delta n_R + j\Delta n_I$ caused by the injection of an electron-hole plasma into a semiconductor [24]. In electronically tunable lasers, this refractive index change induces a blue shift of the wavelength-selective intracavity filter characteristic and hence a blue shift of the laser wavelength. In order to assess the suitability for electronic wavelength tuning at telecom wavelengths, the carrier-induced refractive index and absorption change of InGaAsP (bandgap wavelength 1400 nm), InP and Si are calculated. Hereby the absorption change is given by $\Delta\alpha = -2k_0\Delta n_I$, where $k_0 = 2\pi/\lambda_0$ and $\lambda_0 = 1550\ \text{nm}$. The calculation results are shown in Figs. 1(a) and (b). For a commonly achievable carrier density of $10^{18}\ \text{cm}^{-3}$ the refractive index change of InGaAsP is indeed an order of magnitude larger than for Si. Meanwhile, the carrier-induced absorption change is about half the absorption change of Si. Figure 1(c) shows the ratio of the refractive index change to the absorption coefficient change as a function of carrier density. $-\Delta n_R/\Delta n_I$ is significantly higher in InGaAsP than that in InP and Si, which makes InGaAsP ideal for wavelength tuning based on FCD with relatively low optical loss.

III. LASER CONFIGURATIONS

In this paper, we consider III-V-on-silicon tunable lasers that are based on the integration of a standard InP amplifier epitaxial layer stack on silicon and lasers that make use of

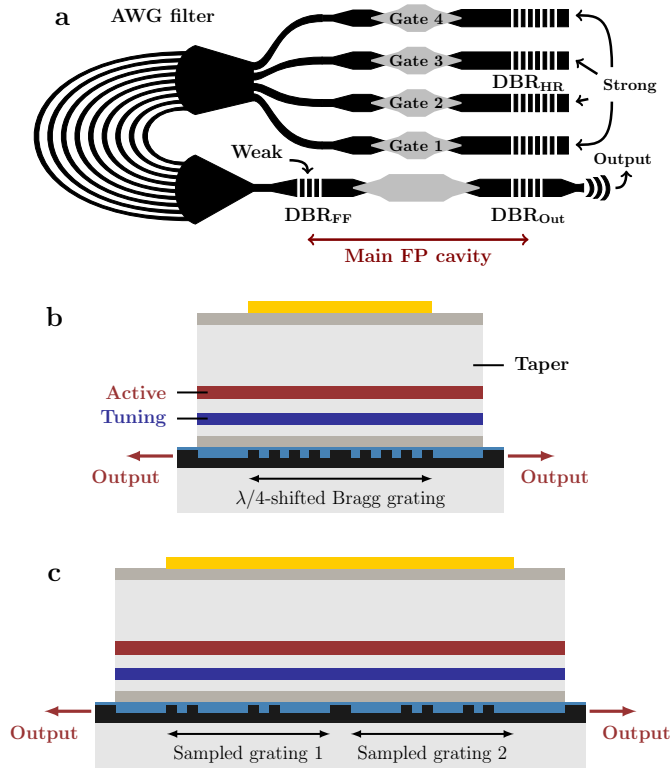


Fig. 3. Overview of the different laser structures. (a) AWG laser with filtered feedback (top view); (b) TTG-DFB laser with uniform grating (side view); (c) TTG-DFB laser with sampled gratings (side view).

a tunable twin-guide (TTG) InP stack on silicon. The latter contains an extra passive tuning layer and constitutes two double heterojunctions with an n -type separation layer that electronically decouples the active and tuning layer. In this way, gain and wavelength can be controlled independently through two control currents. This is illustrated in Figs. 2(a) and (b), which show the typical hybrid waveguide cross-sections for lasers based on the respective stacks.

The fabrication process of the lasers is extensively described in [25], [26] and is based on adhesive divinylsiloxanebis-benzocyclobutene (DVS-BCB) bonding of the InP epitaxy on SOI. After bonding, the InP substrate is removed through wet etching and a SiN_x hard mask is deposited to define the laser mesa (width $\sim 3 \mu\text{m}$). The latter has a V-shape, which enhances the InP-to-silicon coupling in the tapers. Subsequently, the remainder of the laser is fabricated through a combination of dry and wet etching steps. The n -type Ohmic contacts are based on a Ni/Ge/Au metallurgy whereas Ti/Au is used for the p -type Ohmic contacts.

A. Discretely Tunable AWG Laser with Filtered Feedback

The first laser structure is based on the standard InP stack and allows for discrete wavelength tuning for which it relies on delayed optical feedback to the main laser cavity [27]. Using such on-chip optical feedback for wavelength selectivity the lasers are less affected by temperature fluctuations caused by tuning currents, as the tuning sections are located outside the main laser cavity [28]–[30]. A schematic of the laser

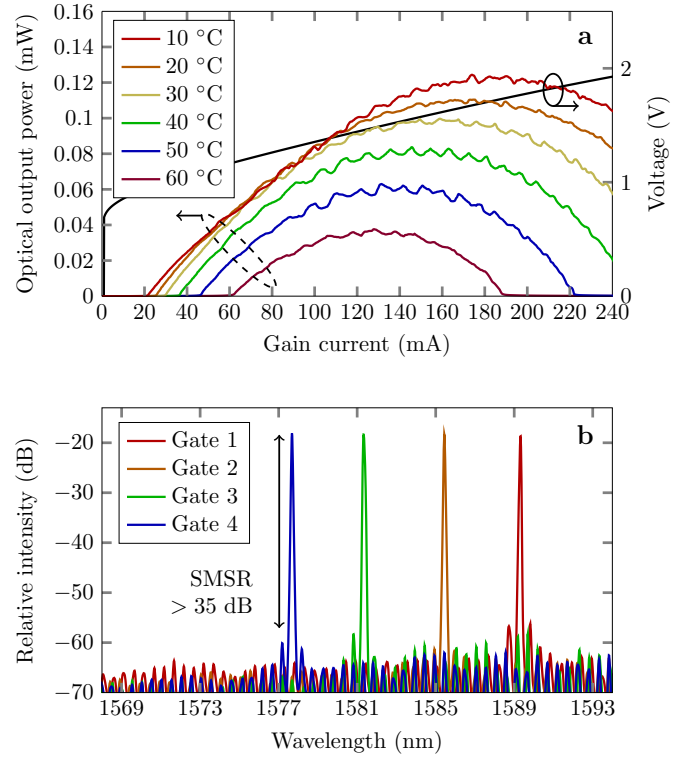


Fig. 4. AWG laser with filtered feedback. (a) LIV characteristics at different substrate temperatures for unbiased gates (fiber-coupled output power); (b) Superimposed laser spectra when the optical gates are appropriately biased above transparency, at a DC gain current of 80 mA and a substrate temperature of 20 °C.

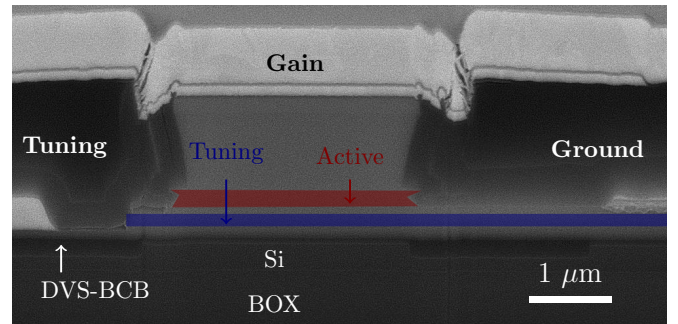


Fig. 5. SEM image of the TTG-DFB laser cross section, captured in the center of the device.

structure is shown in Fig. 3(a). The laser consists of a main Fabry-Pérot (FP) cavity with two partially reflective broadband silicon DBR mirrors (denoted as DBR_{FF} and DBR_{Out} , respectively). At one side of the FP cavity the light output is coupled to an AWG filter that demultiplexes the light in four different waveguide branches. In each branch an InP-on-silicon semiconductor optical amplifier (SOA) is implemented that can function as optical gate. If the SOA is biased at or above transparency, incident light can be efficiently transmitted or even be amplified. When unbiased, all incoming light is absorbed in the gate. By making use of a highly reflective silicon DBR mirror at the end of each waveguide branch (denoted as DBR_{HR}), light is fed back to the laser. This

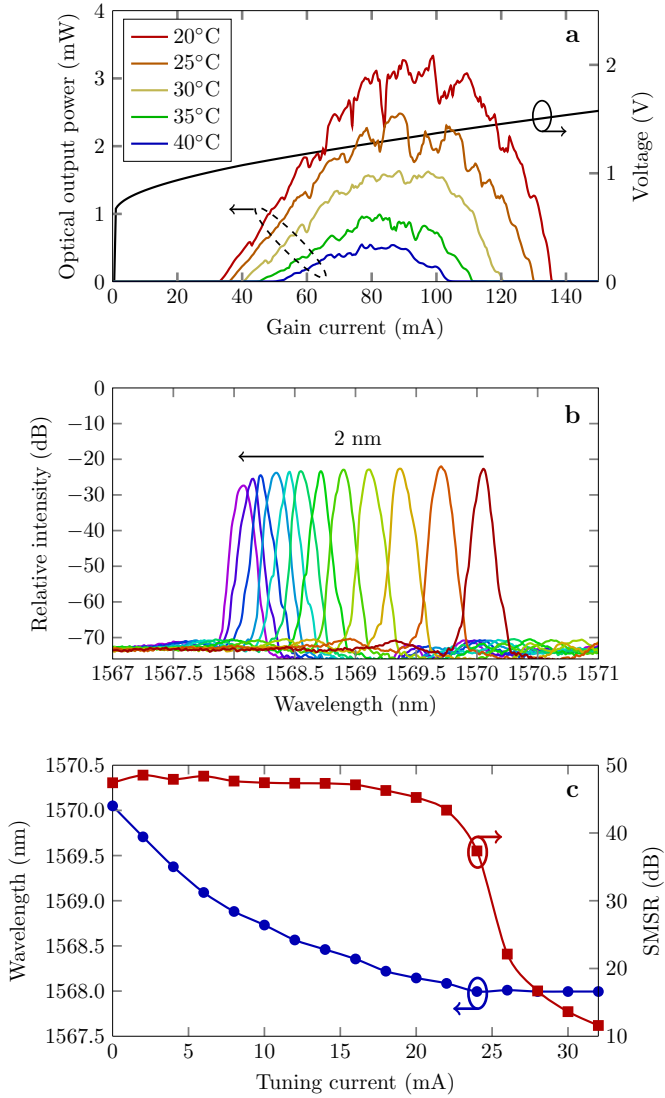


Fig. 6. TTG-DFB laser with uniform grating. (a) LIV characteristics at different substrate temperatures (waveguide-coupled output power); (b) Superimposed laser spectra for tuning currents between 0 and 22 mA (red to purple, steps of 2 mA) at a DC gain current of 90 mA and a substrate temperature of 20°C; (c) Laser wavelength and SMSR versus tuning current for a DC gain current of 90 mA and a substrate temperature of 20°C.

enables the laser to operate in single-mode regime, close to the wavelength selected by the AWG filter [31]–[33]. The straight section lengths of the main FP cavity and optical gates are 240 μm and 40 μm , respectively. For the AWG filter an acyclic design is chosen with 4 output channels, a channel spacing of 4 nm and a free spectral range (FSR) of 20 nm. All silicon DBRs have a waveguide width of 2 μm and are implemented in a 400 nm silicon device layer with 180 nm partial etch depth. The grating period is 252 nm in all DBR reflectors.

The light-current-voltage (LIV) characteristics at different substrate temperatures for unbiased gates are shown in Fig. 4(a). Continuous-wave (CW) laser operation up to 65°C is achieved. The laser threshold is 20 mA at room temperature, with a maximum fiber-coupled output power of 0.1 mW, corresponding to a maximum waveguide-coupled output power of 4 mW. When one of the SOA gates is biased at or above

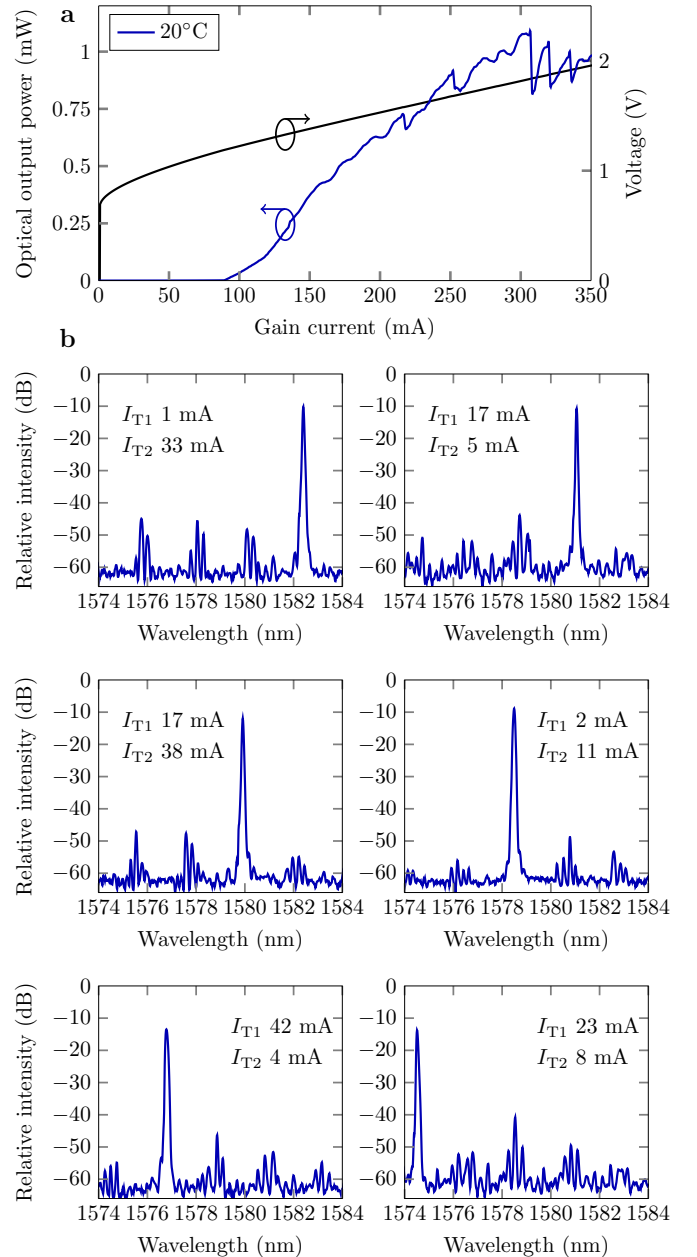


Fig. 7. TTG-DFB laser with sampled gratings. (a) LIV characteristics at a substrate temperature of 20°C (waveguide-coupled output power); (b) Laser spectra at a DC gain current of 300 mA and a substrate temperature of 20°C.

transparency single-mode laser operation can be achieved because of the filtered feedback. Figure 4(b) shows the laser spectra when the gates are appropriately biased, at a gain current of 80 mA. The transparency current varies between 20 mA and 24 mA for the different gates. Single-mode laser operation is achieved with an SMSR larger than 35 dB for all four wavelength channels. The spacing between the channels is 4 nm, which is in line with the AWG design.

B. TTG-DFB Laser with Uniform Grating

Important disadvantages of the AWG laser with filtered feedback are the limited channel scalability and the unsuitability for continuous wavelength tuning. Therefore, a TTG-DFB

laser structure is proposed [26], in which use is made of a TTG epitaxial layer stack with tuning layer that is integrated on top of a quarter-wave ($\lambda/4$)-shifted silicon Bragg grating (Fig. 3(b)). The structure is transversely integrated, such that inherent continuous tunability can be provided [24]. In this design, a tuning layer thickness $t_T = 190$ nm is used as it provides a good trade-off between a sufficiently high grating coupling coefficient $\kappa \approx 115$ cm⁻¹ and a sufficiently large confinement factor in the tuning layer $\Gamma_T \approx 24\%$. The latter is directly proportional to the wavelength tuning efficiency through [24]:

$$\frac{\Delta\lambda_B}{\Delta N} = \Gamma_T \frac{\lambda_B}{n_g} \frac{dn_T}{dN}, \quad (1)$$

where n_g is the group index, λ_B the Bragg wavelength, n_T the refractive index of InGaAsP in the tuning layer and N the carrier density. The first-order Bragg grating has a period of 240 nm and corresponds to a Bragg wavelength of 1570 nm, close to the gain peak of the TTG stack.

A scanning electron microscope (SEM) image of the cross section of a fabricated TTG-DFB laser is shown in Fig. 5. Fabrication is on target, with a DVS-BCB bonding layer thickness of 40 nm and a relatively small spacing between the tuning/ground contact and the laser mesa. The LIV characteristics at different temperatures for a device with a 350 μ m long Bragg grating are shown in Fig. 6(a). At 20°C the threshold current is 33 mA. The maximum fiber-coupled output power is 0.1 mW, which corresponds to a waveguide-coupled output power of about 3 mW. Figure 6(b) shows the superimposed laser spectra for different tuning currents at a fixed gain current of 90 mA. Continuous wavelength tuning is possible over a total tuning range of 2 nm. The blue shift of the laser wavelength for an increased tuning current indicates FCD-based tuning. Apart from a wavelength shift, it also leads to an additional optical loss, as illustrated in Fig. 1(b). Moreover, current injection yields a temperature increase of the active layer because of self-heating, which deteriorates the laser performance and which explains why the laser eventually shuts off. Nevertheless is single-mode laser operation achieved, with an SMSR that remains larger than 44 dB across the tuning range (Fig. 6(c)).

C. TTG-DFB Laser with Sampled Gratings

The use of a uniform Bragg grating inherently limits the wavelength tuning range. By making use of two sampled gratings (SGs) with different sampling periods, the Vernier effect can be exploited to extend the tuning range [34]. A schematic of the laser structure is shown in Fig. 3(c). In this case a design is chosen with sampled gratings that exhibit a mere 2.5 nm and 3 nm peak spacing.

The LIV characteristics of the sampled-grating (SG-) TTG-DFB laser are shown in Fig. 7(a). The laser threshold is 93 mA and a maximum waveguide-coupled output power of 1 mW is obtained. The ripple for gain currents above 300 mA can be attributed to mode hopping. Laser spectra for different tuning currents in the front and back reflector (I_{T1} and I_{T2} , respectively) at a fixed DC gain current of 300 mA are shown in Fig. 7(b). The overall tuning range is around 8 nm and

the SMSR remains within 30 and 40 dB. The limited tuning range is due to the low grating coupling coefficient and the inevitable trade-off in the laser design (confinement in the active layer, tuning layer and silicon waveguide). Extensive improvements in the design and epitaxial layer growth can, however, enhance the modal gain and further extend the overall wavelength tuning range.

IV. DIRECT MODULATION AND WAVELENGTH SWITCHING CHARACTERISTICS

For characterization of the direct modulation behavior, a large-amplitude non-return-to-zero on-off-keying (NRZ-OOK) RF electrical signal is applied to the gain contact of the laser devices at a fixed DC gain current. Through a *p-i-n* photodetector the modulated output is detected in a back-to-back configuration. Eye diagrams for direct modulation of the gain current at 12.5 Gbit/s in the AWG laser with filtered feedback (DC gain current of 80 mA, RF voltage swing of 3 Vpp) and the TTG-DFB laser with uniform grating (DC gain current of 90 mA, RF voltage swing of 2.5 Vpp) are shown in Figs. 8(a) and (b), respectively. Open eye diagrams are obtained, without using any equalization. The length of the SG-TTG-DFB laser prohibits fast direct modulation and requires external modulation.

The wavelength switching characteristics of the laser devices are characterized by applying a large-signal modulated gate/tuning current, at a fixed DC gain current. The light output is then sent through a tunable bandpass filter, such that the laser peak periodically falls within and outside of the filter passband. The power-dependent output levels are monitored with an oscilloscope from which the wavelength switching time can be estimated. The large-signal time-domain wavelength switching characteristics for the AWG laser with filtered feedback and the TTG-DFB laser with uniform grating are shown in Figs. 9(a) and (b), respectively. The AWG laser yields a rise and fall time around 190 ps. For the TTG-DFB laser switching times around 3 ns are obtained (similar switching times are expected for the SG-TTG-DFB laser). It is clear that the obtained switching times in the AWG laser are much shorter than for the TTG-DFB laser. This is due to the stimulated emission process in the optical gates that reduces the carrier lifetime of the injected carriers. This stimulated emission process does not happen when carriers are injected in the passive tuning layer of the TTG stack. We furthermore note that it is possible to implement a thermal drift suppression technique in an array of TTG-DFB lasers, in which the tuning regions of non-lasing lasers are used as heaters for temperature compensation. In this way the total heating remains constant upon switching such that fast and stable wavelength tuning is guaranteed [35].

V. TTG-DBR LASER STRUCTURE

Because of the inherent trade-off between mode confinement in the active, tuning and silicon layer, the tuning range of the TTG-DFB lasers remains limited. Moreover, the waveguide geometry is asymmetric (see Fig. 2(b)), which can lead to a misalignment between the carrier density profile and the

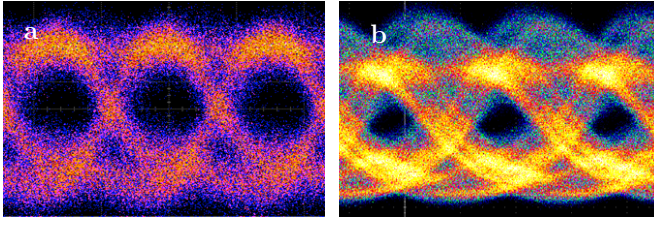


Fig. 8. Eye diagrams under NRZ-OOK direct modulation of the gain current at 12.5 Gbit/s (a) For the AWG laser with filtered feedback; (b) For the TTG-DFB laser with uniform grating.

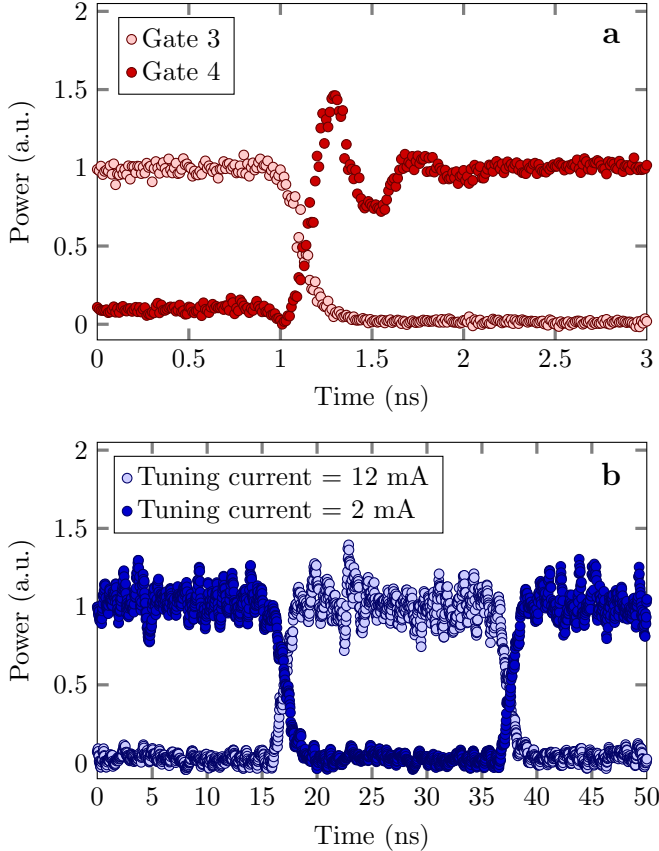


Fig. 9. Large-signal time-domain wavelength switching characteristics. (a) For the AWG laser with filtered feedback (switching between Gate 3 and Gate 4); (b) For the TTG-DFB laser with uniform grating.

optical mode. It also causes strong lateral carrier diffusion in the tuning layer, away from the optical mode. Therefore, a novel TTG-DBR laser structure is proposed. The structure is shown in Fig. 10 and consists of several longitudinal sections: a Gain, Phase and Bragg section and two taper sections to couple the light down from the Gain section. In the Gain section, only the active layer is biased and the tuning layer is left unbiased. Wavelength-selective feedback is provided in the Bragg section, which can be tuned through current injection into the tuning layer. The Phase section is used to prevent mode hopping upon wavelength tuning. The TTG-DBR laser structure offers the possibility for separate optimization of each longitudinal laser section, as opposed to the TTG-DFB laser structure. More in particular, the following

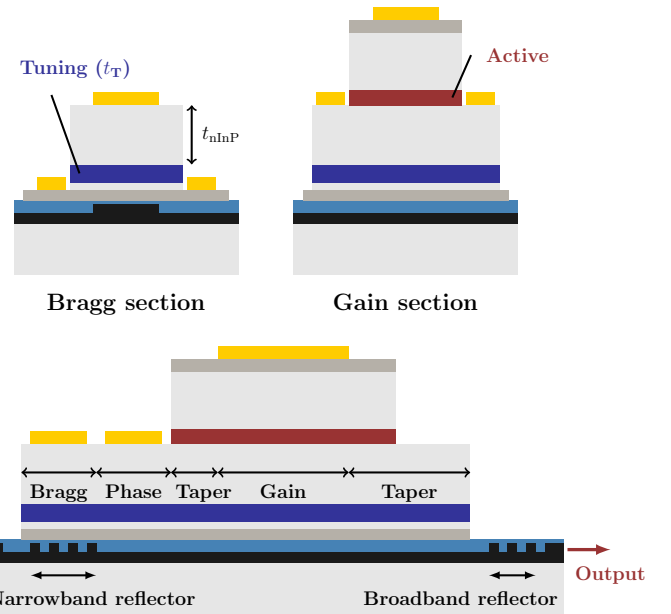


Fig. 10. Schematic of the TTG-DBR laser structure (longitudinal view). Cross-sectional views of the Bragg and Gain section are shown as well.

design improvements are made: first, the use of a much thicker tuning layer (thickness t_T) can significantly enhance the optical confinement factor in the tuning layer, in turn enhancing the wavelength tuning range and efficiency. Second, a very thick n -type InP cladding layer (thickness $t_{n\text{InP}}$) can allow for a symmetric waveguide cross section with the n -type metal contact placed on top of the tuning waveguide. This cross-sectional symmetry in both the Bragg and Phase section offers the advantage that the tuning waveguide is well-defined and laterally limited in space, which prevents carrier out diffusion in the tuning layer. It also ensures that the modal overlap with the injected carriers is optimal. Note that the use of such a thick n -InP layer has important consequences for light coupling between the Gain section, the Bragg and Phase section and the silicon output waveguide. In [36] an adiabatic tapered coupler is discussed that could form the basis as coupler for this laser structure. The following sections discuss the optimum choice for the tuning layer and n -InP cladding layer thickness.

A. Optimization of the Tuning Layer Thickness

The influence of the tuning layer thickness t_T on the confinement factor in the tuning layer Γ_T and the grating coupling coefficient κ is shown in Figs. 11(a) and (b), respectively. Thereby a p -InGaAsP contact layer thickness $t_C = 150$ nm and DVS-BCB thickness $t_{\text{DVS-BCB}} = 50$ nm is assumed. The former is slightly thicker than for the TTG-DFB laser, where a more difficult trade-off between the confinement in the different sections is in place. Clearly Γ_T dramatically increases with increasing t_T . Furthermore, $t_{n\text{InP}}$ seems to have little influence on both Γ_T and κ for $t_T > 200$ nm. A tuning layer thickness $t_T = 225$ nm seems an adequate choice, with $\Gamma_T \approx 0.4$ and $\kappa \approx 200 \text{ cm}^{-1}$. The increased confinement factor in the tuning layer is expected to yield a close to

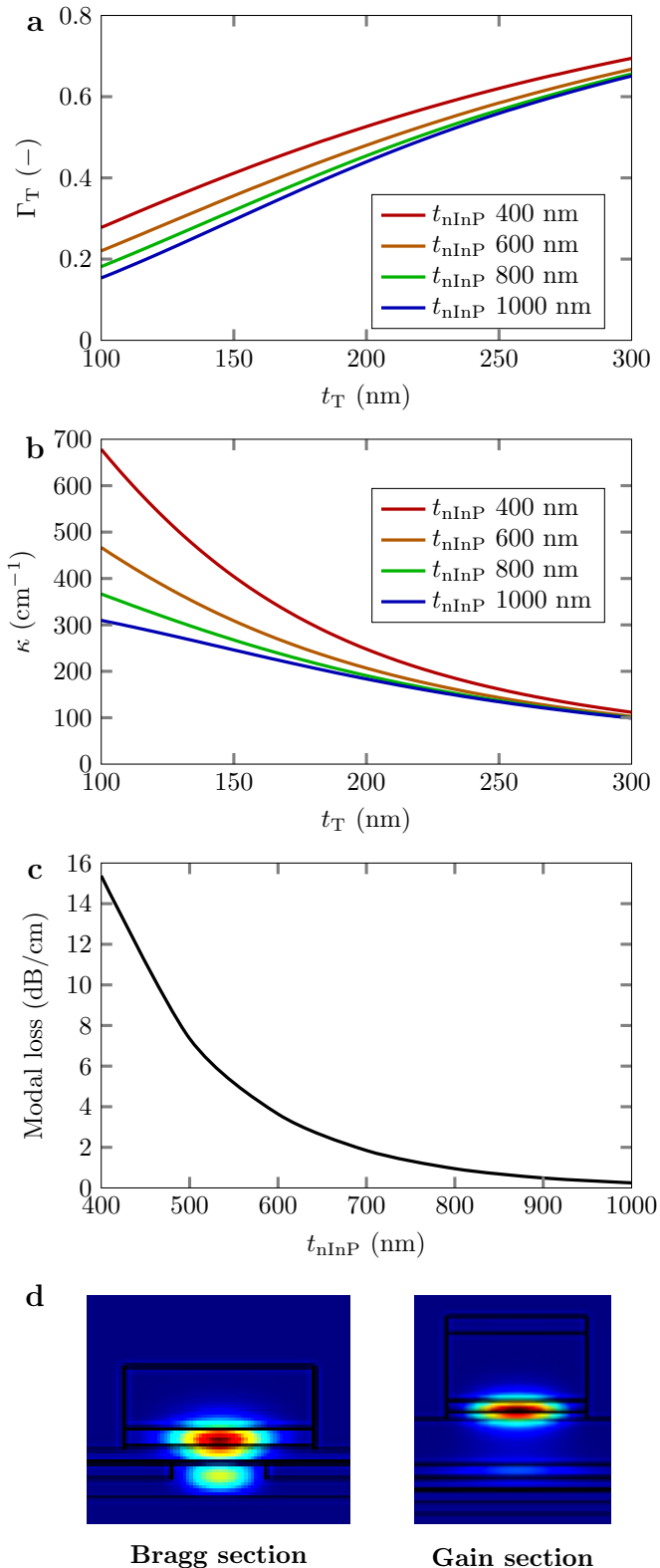


Fig. 11. Optimization of the tuning and cladding layer thickness. (a) Influence of t_T on the confinement factor in the tuning layer Γ_T ; (b) Influence of t_T on the grating coupling coefficient κ ; (c) Influence of t_{nInP} on the modal loss, with assumption of a Ni/Ge/Au metallurgy; (d) Optical mode profiles in the Bragg and Gain section for the optimized design.

factor 2 improvement in the overall wavelength tuning range

as compared to tuning range of the TTG-DFB laser.

B. Optimization of the Cladding Layer Thickness

Although the thickness of the n -InP cladding layer has some influence on Γ_T and t_T , a more stringent condition is put by the absorption loss when a metal contact is defined on top of the mesa. Figure 11(c) shows the simulated modal loss versus t_{nInP} . Thereby a Ni/Ge/Au metallurgy is assumed. A thickness $t_{nInP} > 800$ nm seems a good choice, with a modal loss that remains below 2 dB/cm. Obviously, t_{nInP} cannot be chosen too large either, as it would dramatically increase the length of the coupling structure. The optical mode profiles in the Bragg and Gain section for the optimized design are shown in Fig. 11(d).

VI. CONCLUSION

In this paper, we have discussed a set of distinct electronically tunable laser structures heterogeneously integrated on a silicon photonics platform. The emphasis is on fast wavelength tuning, which is realized through a tunable twin-guide epitaxial layer stack, enabled by the very strong free-carrier plasma dispersion effect in InGaAsP. Related tuning mechanisms based on carrier-depletion or tuning in silicon cannot easily lead to comparable laser characteristics. Dynamic wavelength modulation experiments indicate wavelength switching times of about 3 ns and even below 1 ns for an AWG laser with discrete wavelength selectivity based on filtered feedback. Albeit not continuously tunable, the latter can be of particular interest as the laser design can easily be matched with the AWG grid of the deployed passive filter in the routing network. Finally, we have proposed and designed a TTG-DBR laser that combines nanosecond wavelength tuning with a large tuning efficiency and range. The presented laser devices can be attractive candidates for optical packet switching applications in data center networks.

ACKNOWLEDGMENT

The authors would like to thank R. Meyer and A. Königer for providing the TTG epitaxy and L. Van Landschoot, S. Verstyft and M. Muneeb for technical support.

REFERENCES

- [1] C. V. Networking, "Cisco global cloud index: forecast and methodology, 2016-2021. white paper," *Cisco Public*, 2018.
- [2] D. J. Blumenthal, J. Barton, N. Beheshti, J. E. Bowers, E. Burmeister, L. A. Coldren, M. Dummer, G. Epps, A. Fang, Y. Ganjali, J. Garcia, B. Koch, V. Lal, E. Lively, J. Mack, M. Masanovi, N. McKeown, K. Nguyen, S. C. Nicholes, H. Park, B. Stamenic, A. Tauke-Pedretti, H. Poulsen, and M. Sysak, "Integrated photonics for low-power packet networking," *IEEE Journal of Selected Topics in Quantum Electronics*, vol. 17, no. 2, pp. 458–471, March 2011.
- [3] A. Wonfor, H. Wang, R. Penty, and I. White, "Large port count high-speed optical switch fabric for use within datacenters," *Journal of Optical Communications and Networking*, vol. 3, no. 8, pp. A32–A39, 2011.
- [4] T. S. El-Bawab, *Optical switching*. Springer Science & Business Media, 2008.
- [5] M. Chen, H. Jin, Y. Wen, and V. C. Leung, "Enabling technologies for future data center networking: a primer," *IEEE Network*, vol. 27, no. 4, pp. 8–15, 2013.

- [6] D. Taillaert, F. Van Laere, M. Ayre, W. Bogaerts, D. Van Thourhout, P. Bienstman, and R. Baets, "Grating couplers for coupling between optical fibers and nanophotonic waveguides," *Japanese Journal of Applied Physics*, vol. 45, no. 8R, p. 6071, 2006.
- [7] X. Wang, W. Shi, H. Yun, S. Grist, N. A. Jaeger, and L. Chrostowski, "Narrow-band waveguide bragg gratings on SOI wafers with CMOS-compatible fabrication process," *Optics Express*, vol. 20, no. 14, pp. 15 547–15 558, 2012.
- [8] J. Niehusmann, A. Vörckel, P. H. Bolivar, T. Wahlbrink, W. Henschel, and H. Kurz, "Ultra-high-quality-factor silicon-on-insulator microring resonator," *Optics Letters*, vol. 29, no. 24, pp. 2861–2863, 2004.
- [9] T. Fukazawa, F. Ohno, and T. Baba, "Very compact arrayed-waveguide-grating demultiplexer using Si photonic wire waveguides," *Japanese Journal of Applied Physics*, vol. 43, no. 5B, p. L673, 2004.
- [10] P. D. Dobbelaere, A. Dahl, A. Mekis, B. Chase, B. Weber, B. Welch, D. Foltz, G. Armijo, G. Masini, G. McGee, G. Wong, J. Balardeta, J. Dotson, J. Schramm, K. Hon, K. Khauv, K. Robertson, K. Stechschulte, K. Yokoyama, L. Planchon, L. Tullgren, M. Eker, M. Mack, M. Peterson, N. Rudnick, P. Milton, P. Sun, R. Bruck, R. Zhou, S. Denton, S. Fath-pour, S. Gloeckner, S. Jackson, S. Pang, S. Sahni, S. Wang, S. Yu, T. Pinguet, Y. D. Koninck, Y. Chi, and Y. Liang, "Advanced silicon photonics technology platform leveraging a semiconductor supply chain," in *2017 IEEE International Electron Devices Meeting (IEDM)*, Dec 2017, pp. 34.1.1–34.1.4.
- [11] R. Soref, "The past, present, and future of silicon photonics," *IEEE Journal of Selected Topics in Quantum Electronics*, vol. 12, no. 6, pp. 1678–1687, 2006.
- [12] G. Duan, C. Jany, A. L. Liepvre, A. Accard, M. Lamponi, D. Make, P. Kaspar, G. Levaufré, N. Girard, F. Lelarge, J. Fedeli, A. Descos, B. B. Bakir, S. Messaoudene, D. Bordel, S. Menezes, G. de Valicourt, S. Keyvaninia, G. Roelkens, D. V. Thourhout, D. J. Thomson, F. Y. Gardes, and G. T. Reed, "Hybrid III–V on silicon lasers for photonic integrated circuits on silicon," *IEEE Journal of Selected Topics in Quantum Electronics*, vol. 20, no. 4, pp. 158–170, July 2014.
- [13] G. Roelkens, L. Liu, D. Liang, R. Jones, A. Fang, B. Koch, and J. Bowers, "III–V/silicon photonics for on-chip and intra-chip optical interconnects," *Laser & Photonics Reviews*, vol. 4, no. 6, pp. 751–779, 2010.
- [14] T. Komljenovic, M. Davenport, J. Hulme, A. Y. Liu, C. T. Santis, A. Spott, S. Srinivasan, E. J. Stanton, C. Zhang, and J. E. Bowers, "Heterogeneous silicon photonic integrated circuits," *Journal of Lightwave Technology*, vol. 34, no. 1, pp. 20–35, 2016.
- [15] G. P. Agrawal, *Fiber-optic communication systems*. John Wiley & Sons, 2012, vol. 222.
- [16] T. Komljenovic, L. Liang, R.-L. Chao, J. Hulme, S. Srinivasan, M. Davenport, and J. E. Bowers, "Widely-tunable ring-resonator semiconductor lasers," *Applied Sciences*, vol. 7, no. 7, p. 732, 2017.
- [17] T. Ferrotti, B. Blampey, C. Jany, H. Duprez, A. Chantre, F. Boeuf, C. Seassal, and B. B. Bakir, "Co-integrated 1.3 μm hybrid III–V/silicon tunable laser and silicon Mach-Zehnder modulator operating at 25Gb/s," *Optics Express*, vol. 24, no. 26, pp. 30 379–30 401, 2016.
- [18] S. Dhoore, L. Li, A. Abbasi, G. Roelkens, and G. Morthier, "Demonstration of a discretely tunable III–V-on-silicon sampled grating DFB laser," *IEEE Photonics Technology Letters*, vol. 28, no. 21, pp. 2343–2346, 2016.
- [19] S. Dhoore, G. Roelkens, and G. Morthier, "III–V-on-silicon three-section DBR laser with over 12 nm continuous tuning range," *Optics Letters*, vol. 42, no. 6, pp. 1121–1124, 2017.
- [20] G. T. Reed, G. Mashanovich, F. Y. Gardes, and D. Thomson, "Silicon optical modulators," *Nature Photonics*, vol. 4, no. 8, p. 518, 2010.
- [21] M. N. Sysak, J. O. Anthes, D. Liang, J. E. Bowers, O. Rada, and R. Jones, "A hybrid silicon sampled grating DBR tunable laser," in *Group IV Photonics, 2008 5th IEEE International Conference on*. IEEE, 2008, pp. 55–57.
- [22] D. Liang, X. Huang, G. Kurczveil, M. Fiorentino, and R. Beausoleil, "Integrated finely tunable microring laser on silicon," *Nature Photonics*, vol. 10, no. 11, p. 719, 2016.
- [23] T. Verolet, A. Gallet, X. Pommared, J. Decobert, D. Make, J.-G. Provost, M. Fournier, C. Jany, S. Olivier, A. Shen, and G. Duan, "Hybrid III–V on silicon fast and widely tunable laser based on rings resonators with PIN junctions," in *Asia Communications and Photonics Conference*. IEEE, 2018.
- [24] J. Buus, M.-C. Amann, and D. J. Blumenthal, *Tunable laser diodes and related optical sources*. Wiley-Interscience New York, 2005.
- [25] G. Roelkens, A. Abassi, P. Cardile, U. Dave, A. de Groote, Y. de Koninck, S. Dhoore, X. Fu, A. Gassenq, N. Hattasan, Q. Huang, S. Kumari, S. Keyvaninia, B. Kuyken, L. Li, P. Mechet, M. Muneeb, D. Sanchez, H. Shao, T. Spuesens, A. Z. Subramanian, S. Uvin, M. Tassaert, K. van Gasse, J. Verbist, R. Wang, Z. Wang, J. Zhang, J. van Campenhout, X. Yin, J. Bauwelinck, G. Morthier, R. Baets, and D. van Thourhout, "III–V-on-silicon photonic devices for optical communication and sensing," *Photonics*, vol. 2, no. 3, pp. 969–1004, 2015.
- [26] S. Dhoore, A. Königinger, R. Meyer, G. Roelkens, and G. Morthier, "Electronically tunable distributed feedback (DFB) laser on silicon," *Laser & Photonics Reviews*, vol. 13, no. 3, p. 1800287, 2019.
- [27] S. Dhoore, A. Rahim, G. Roelkens, and G. Morthier, "12.5 Gbit/s discretely tunable InP-on-silicon filtered feedback laser with sub-nanosecond wavelength switching times," *Optics Express*, vol. 26, no. 7, pp. 8059–8068, 2018.
- [28] S. Matsuo, T. Segawa, T. Kakitsuka, T. Sato, R. Takahashi, H. Suzuki, B. Docter, F. Karouta, and M. Smit, "Integrated filtered feedback tunable laser using double-ring-resonator-coupled filter," in *Semiconductor Laser Conference, 2008. ISLC 2008. IEEE 21st International*. IEEE, 2008, pp. 155–156.
- [29] B. Docter, J. Pozo, S. Beri, I. V. Ermakov, J. Danckaert, M. K. Smit, and F. Karouta, "Discretely tunable laser based on filtered feedback for telecommunication applications," *IEEE Journal of Selected Topics in Quantum Electronics*, vol. 16, no. 5, pp. 1405–1412, 2010.
- [30] S. Furst, S. Yu, and M. Sorel, "Fast and digitally wavelength-tunable semiconductor ring laser using a monolithically integrated distributed Bragg reflector," *IEEE Photonics Technology Letters*, vol. 20, no. 23, pp. 1926–1928, 2008.
- [31] A. P. Fischer, O. K. Andersen, M. Yousefi, S. Stolte, and D. Lenstra, "Experimental and theoretical study of filtered optical feedback in a semiconductor laser," *IEEE Journal of Quantum Electronics*, vol. 36, no. 3, pp. 375–384, 2000.
- [32] D. M. Kane and K. A. Shore, *Unlocking dynamical diversity: optical feedback effects on semiconductor lasers*. John Wiley & Sons, 2005.
- [33] H. Erzgräber and B. Krauskopf, "Dynamics of a filtered-feedback laser: influence of the filter width," *Optics Letters*, vol. 32, no. 16, pp. 2441–2443, 2007.
- [34] R. Todt, T. Jacke, R. Meyer, J. Adler, R. Laroy, G. Morthier, and M.-C. Amann, "Sampled grating tunable twin-guide laser diodes with over 40-nm electronic tuning range," *IEEE Photonics Technology Letters*, vol. 17, no. 12, pp. 2514–2516, 2005.
- [35] N. Nunoya, H. Ishii, Y. Kawaguchi, R. Iga, T. Sato, N. Fujiwara, and H. Oohashi, "Tunable distributed amplification (TDA-) DFB laser with asymmetric structure," *IEEE Journal of Selected Topics in Quantum Electronics*, vol. 17, no. 6, pp. 1505–1512, 2011.
- [36] S. Dhoore, S. Uvin, D. Van Thourhout, G. Morthier, and G. Roelkens, "Novel adiabatic tapered couplers for active III–V/SOI devices fabricated through transfer printing," *Optics Express*, vol. 24, no. 12, pp. 12 976–12 990, 2016.



Sören Dhoore received the M.Sc. degree and the Ph.D. degree in photonics engineering from Ghent University, Ghent, Belgium, in 2014 and 2018, respectively. His current research interests include heterogeneously integrated tunable lasers for telecommunication and sensing applications. He is a member of the IEEE Photonics Society and the Optical Society (OSA).



Gunther Roelkens received the degree in electrical engineering and the Ph.D. degree from the Department of Information Technology (INTEC), Ghent University, Ghent, Belgium, in 2002 and 2007, respectively, where he is currently an Associate Professor. In 2008, he was a Visiting Scientist with the IBM T. J. Watson Research Center, Rochester, NY, USA. He is an Assistant Professor with Eindhoven University of Technology, Eindhoven, The Netherlands. His research interests include the heterogeneous integration of III-V semiconductors and

other materials on top of silicon waveguide circuits and electronic/photonic cointegration. He was holder of an ERC starting grant (MIRACLE), to start up research in the field of integrated mid-infrared photonic integrated circuits.



Geert Morthier received the degree in electrical engineering and the Ph.D. degree from Ghent University, Ghent, Belgium, in 1987 and 1991, respectively. Since 1991, he has been a member of the permanent staff of imec. His main interests include the modeling and characterization of optoelectronic components. He has authored or co-authored more than 150 papers in the field and holds several patents. He is also one of the two authors of the Handbook of Distributed Feedback Laser (Artech House, 1997). From 1998 to end of 1999, he was the Project

Manager of the ACTS Project ACTUAL dealing with the control of widely tunable laser diodes, from 2001 to 2005, he was the Project Manager of the IST Project NEWTON on new widely tunable lasers, and from 2008 to 2011, he was the Project Manager of the FP7 Project HISTORIC on microdisk lasers. In 2001, he was appointed Part-time Professor at Ghent University, where he teaches courses on optical fiber communication and lasers.